



**Bacterial Growth Monitored by Two-Dimensional Tandem
Mass Spectrometry**

Journal:	<i>Analyst</i>
Manuscript ID	AN-ART-10-2021-001901.R1
Article Type:	Paper
Date Submitted by the Author:	28-Jan-2022
Complete List of Authors:	Szalwinski, Lucas; Purdue University Department of Chemistry, Chemistry Gonzalez, L. Edwin; Purdue University, Chemistry Morato, Nicolás; Purdue University, Chemistry Marsch, Brett; Purdue University Department of Chemistry, Chemistry Cooks, R. Graham; Purdue University, Chemistry

Bacterial Growth Monitored by Two-Dimensional Tandem Mass Spectrometry

Lucas J. Szalwinski; L. Edwin Gonzalez; Nicolás M. Morato; Brett M. Marsh; R. Graham Cooks*

Purdue University Department of Chemistry, West Lafayette, IN 47907

*email: cooks@purdue.edu

Abstract

The growth of the bacterium *E. coli* was monitored by targeting the phospholipid constituents through desorption electrospray ionization and characterizing individual sets of isomers by recording the full 2D MS/MS data domain in a single scan of a modified quadrupole ion trap mass spectrometer. The experiments tested the applicability of the new instrumental capabilities which include sample interrogation at the molecular level for multiple components at speeds of <10 seconds/sample. The major lipids observed were phosphatidylethanolamines and phosphatidylglycerols and the growth experiment showed fatty acid chain modification from alkene to cyclopropyl groups over time. Notably, these novel MS scans were also performed using desorption electrospray ionization (DESI) to quickly sample complex mixtures without pre-separation. This demonstration experiment has implications for the value of ambient ionization mass spectrometry for monitoring biological systems on physiologically relevant timescales.

Keyword: High throughput experiments; Phospholipids; Ambient ionization; Desorption electrospray ionization; Cyclopropyl fatty acids

Introduction

A molecular understanding of biological systems is a fundamental driver in bioanalytical chemistry, particularly when temporal information is also sought. Several choices need to be made to obtain such information: first there is the choice of a signifying class of molecules, as comprehensive analysis is beyond reach. If the biological system is taken to be a bacterial colony, then lipids might be chosen for their chemical diversity and their many roles in the cellular functions of bacteria.¹⁻³ The high dimensionality of phospholipids - in the sense of a large number of closely related molecular structures - is a key advantage of this choice is that different states of the biological system can be expressed in great detail in such a complex array of molecules.⁴⁻⁶ The potential of this approach is clear from that fact that answers to simple questions – diseased/ healthy – are readily read out from the lipid profiles of higher organisms, as in brain cancer diagnostics from phospholipid profiles.⁷ With the organism and target class now selected, the read-out method must be chosen. The usual numerical criteria of chemical analysis, expressed as analytical sensitivity and specificity and dynamic range and quantitative accuracy and precision, all apply. But having chosen lipids and the scale of the experiment, as well as the need to measure many related molecules, only methods based on mass spectrometry (MS) need be considered further. Spectroscopic measurements can broadly detect lipid composition, and in some cases follow individual molecular species in 3D⁸ and in vivo⁹⁻¹¹ and they have naturally excellent time resolution^{12,13}, but they fall short in their broad applicability in specific molecular recognition. The most widely used MS method of assessing the lipid content of a cell is by liquid chromatography tandem mass spectrometry (LC-MS/MS).^{14,15} This method typically requires sample preparation followed by a chromatographic run where the elute is monitored over time by a mass spectrometer. The sample preparation required by this method is not strictly necessary for the analysis of bacterial lipids by desorption electrospray ionization (DESI).^{16,17} The LC-MS/MS method is often acceptable except when a molecular understanding of an organism or cell requires rapid time-dependent information on the molecular composition, i.e. where rapid temporal changes in lipid distributions are needed to signal the biological state.¹⁸⁻²⁰

Direct mass spectrometry of a complex sample is most commonly performed using data-dependent acquisition where only the most abundant ions in the single stage MS are fragmented to provide structural information. Low-abundance ions are ignored in this approach. Data-independent acquisition methods^{21,22} avoid this issue by analyzing all precursor ions. In this experiment individual precursor ions are mass-selected in turn and fragmented. The precursor ion m/z is correlated to chromatographic retention time. The result is a set of MS/MS spectra acquired relatively slowly due to the requisite chromatographic separation prior to the mass spectrometer.

An alternative is to record, in a single scan, all products of all precursors (the full 2D MS/MS data domain) by utilizing the special properties of ion traps. Such an experiment was first demonstrated for a

1
2
3 Fourier transform ion cyclotron resonance spectrometer (FT-ICR).^{23,24} We have used a quadrupole ion
4 trap for the same purpose, activating a set of trapped precursor ions with a dipolar set of ramped
5 frequencies while rapidly scanning product ions to the detector in an orthogonal direction with a second
6 dipolar frequency ramp. Using this approach, we identified the components of mixtures of proscribed
7 drugs.²⁵ Such experiments have two further advantages for the problem at hand: (i) the MS scan can be
8 performed on the 1 Hz time scale and (ii) with appropriate ionization methods no sample preparation is
9 needed.
10
11
12
13

14 In this study we seek to demonstrate a modest version of the general problem laid out in this
15 Introduction: we seek to demonstrate the ability to monitor the changing lipid profile of *E. coli* as a
16 *function of growth time*. The degree of chemical detail in glycerophospholipids is remarkable as there are
17 isomers associated with differences in the fatty acid chain lengths, double bond position, and substitution
18 position on the glycerol for ions at a single *m/z* value.²⁶ New methods have been developed to distinguish
19 lipids at this very high degree of chemical detail.²⁷⁻²⁹ Without seeking to utilize this extra dimension of
20 information, we demonstrate the potential to solve the larger problem by showing direct analysis by DESI
21 using a repetition time of under 10 seconds to acquire the full 2D MS/MS data domain.
22
23
24
25
26
27

28 **Experimental**

29 *E. Coli Culture Conditions and Optical Density Measurements*

30
31 *Escherichia coli* was provided by bioMérieux, Inc. (Hazelwood, MO). The initial cell
32 concentration at the point of inoculation was 4.3×10^7 cells/mL and the culture was incubated at 37 °C,
33 aerobically, in 200 mL of LB broth. To monitor the growth of *E. coli*, aliquots were taken at various times
34 over an 8-hour period. The OD₆₀₀ of the aliquots were measured with a UV-vis spectrophotometer. Two
35 time-intervals were used while making measurements over the 8h growth period; 3 – 30 min intervals
36 during the lag and during the stationary phases, and 22 – 15 min intervals in the time range in which we
37 suspected the exponential phase to occur. Duplicate OD₆₀₀ measurements were taken for each point. The
38 MS measurements were made using nano electrospray ionization (nESI).
39
40
41
42
43

44 A subsequent set of experiments used DESI-MS to analyze lipids in *E. coli*, initial concentration
45 of 3.35×10^8 cells/mL in a culture incubated at 37 °C aerobically in 50 mL of LB broth. Aliquots were
46 taken every 30 minutes until 20 samples had been collected. This was done for three biological replicates.
47 Aliquots were transferred into a 96-well plate and their absorbances were measured in triplicate by a
48 BioTek Synergy 2 microplate reader (Winooski, Vermont USA). Each biological replicate absorbance
49 measurement was taken in triplicate.
50
51
52
53
54

55 *2D MS/MS Measurements*

1
2
3 For nano-electrospray (nESI) measurements, aliquots of suspended *E. coli* were taken from the
4 same stocks used for the optical density measurements to monitor the growth curve. The cell
5 concentration of the first and last time point were determined by hemocytometry to correlate optical
6 density and cell concentration. A constant number of cells were profiled (9×10^7 cells or ~ 100 μg dry
7 weight of cells) for each time point. The cell aliquots were taken directly from the cell culture and
8 centrifuged to separate the cells from the growth medium. Ethanol was then added to the cell pellet to lyse
9 the cells and the corresponding lysate was sprayed without prior workup to record nESI mass spectra.
10
11
12
13

14 The nESI 2D MS/MS scans were performed by trapping precursor ions in a modified LTQ mass
15 spectrometer (Thermo Fisher) with an externally controlled RF trapping voltage.³⁰ The 2D MS/MS scan
16 was performed in 900 milliseconds with precursor ions of m/z 600 – 900 being fragmented by one
17 waveform while the resulting fragment (product) ions were continuously ejected using a second
18 waveform as described previously.³¹ A depiction of the methodology can be found in the Supplemental
19 Information (Figure S1). Twenty-five averages were recorded for each replicate and three replicates were
20 performed for each time point. The raw data (.txt files) were processed in MATLAB and the data requires
21 no computationally intensive pre-processing meaning the 2D MS/MS spectra can be plotted nearly
22 instantaneously.
23
24
25
26
27
28
29

30 *DESI-2D MS/MS measurements*

31 Cell concentrations were determined by the same method as described above. An equivalent
32 number of cells (1.6×10^8) were taken from each aliquot and lipids were extracted using the Bligh and
33 Dyer method.³² From each extract, 10 μL of solution (equivalent to 4×10^7 cells) was deposited onto an
34 individual well of a Teflon-coated 12-well glass microscope slide and allowed to dry. This was done
35 manually for each biological replicate for a total of 60 samples. Samples were analyzed by DESI using a
36 Prosolia DESI 2D system (Indianapolis, IN). Methanol Chromasolv LC-MS grade (Riedel-de Haën -
37 Honeywell, Muskegon, MI) was used as spray solvent for all experiments. The DESI spray voltage was
38 set to -5 kV. Nitrogen (150 psi) was used as nebulizing gas. The emitter distance and DESI spray angle
39 were fixed at ~ 1 mm and 55° , respectively. Secondary ions formed by DESI were injected into the ion
40 trap for 200 milliseconds, followed by a 300-millisecond 2D MS/MS scan focused on the lipid mass
41 region. Each 2D MS/MS mass spectrum consisted of 25 averages for a total analysis time of 12.5
42 seconds/sample. Each biological replicate was run in triplicate resulting in 180 2D MS/MS mass spectra
43 acquired in under 40 minutes.
44
45
46
47
48
49
50
51
52
53

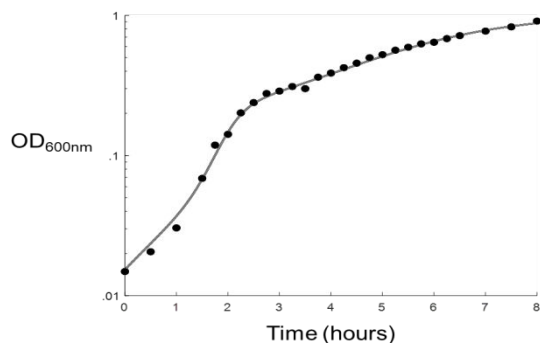
54 *Automated DESI-2D MS/MS measurements*

1
2
3 Aliquots of *E. coli* after 48 hours of growth were centrifuged, the supernatant was removed, and
4 the resulting pellet was dissolved in ethanol. The cell lysate was deposited on four wells within a Teflon-
5 coated 12-well glass microscope slide. Each well was analyzed automatically for approximately 5
6 seconds. Automated DESI was carried out using identical analysis conditions as described above but by
7 controlling the stage motion using the Omni Spray 2D Ion Source Automation software (Prosolia,
8 Indianapolis, IN). The microscope slide was located on the slide holder of the DESI stage, and the
9 positions of the wells were calibrated prior to analysis. An automated *point-to-point oscillatory* motion
10 profile centered in turn on each of the wells was used to define the stage motion. The screening rate and
11 the number of oscillations were manually adjusted to cover the spot diameter in ca. 5 seconds. The slide
12 was located on the stage the analysis proceeded automatically.
13
14
15
16
17
18
19

20 **Results and Discussion**

21 *Bacterial Growth Monitored by Optical Density*

22 The biological system (bacteria), target molecular class (lipids), and read-out system (2D
23 MS/MS) have been chosen. A demonstration of the capabilities laid out in the Introduction requires that
24 the bacterial samples have rich lipidomic features that change over time. A simple version of this
25 experiment is to simply allow the bacteria to grow under favorable conditions and extract aliquots over
26 time. Because bacterial growth is slow the fast-analytical response available in 2D MS/MS is not strictly
27 required. The *E. coli* growth curve is shown in **Figure 1**.
28
29
30
31
32



45 **Figure 1.** Optically measured growth curve of *E. coli* in LB
46 medium at 37 °C

47 Examination of the growth curve shows three distinct phases. The lag phase, in which slow initial
48 growth is observed, occurs within the first hour. The exponential phase occurs from roughly the first hour
49 to three hours while the stationary phase continues until the end of the monitoring. A similar growth
50 curve³³ has been reported using similar culturing conditions. Because it was expected that the greatest
51 changes observed 2D MS/MS data domain would occur during the exponential and lag phases, sampling
52
53
54
55
56
57
58
59
60

was conducted every 30 minutes from 0 to 1.5 hours, 15 minutes from 1.5 hours to 3.5 hours, and intermittently from 3.5 hours to 8 hours.

E. coli Lipid Profile over Time Monitored by nano-electrospray-2D MS/MS

Representative 2D MS/MS data for the three growth phases are shown in **Figure 2**. The 2D MS/MS data domain has three axes, a precursor m/z axis, a product m/z axis, and an intensity axis. The precursor m/z axis value gives the m/z of the precursor ion which is then fragmented, while the product ion m/z axis value gives the m/z values of the fragments of the precursor ions. Negatively-charged phosphatidyl ethanolamine (PE) and phosphatidylglycerol (PG) ions (the most abundant ions observed) primarily produce fragments of their constituent fatty acid chains (m/z 200 - 400). Such information, which is required for structural identification, cannot be obtained in a single-stage MS experiment, while conventional MS/MS product ion scans would need to be performed individually. The 2D MS/MS scan provides this information with a 1 second scan. In the discussion of 2D MS/MS data which follows, the coordinates for 2D MS/MS points will be given as (precursor m/z , product m/z), meaning that the m/z 255 product ion associated with precursor m/z 688, written in the text as (688, 255).

Examination of the 2D MS/MS data domains reveals, as its most prominent feature, the increasing intensity and complexity in the lipid region going from 1.75 hour to 5.25 hour. The strongest features in the early exponential phase are observed at (688, 255), (719, 255), (719, 283), (747, 255) and (747, 283). These combinations of precursor and product ions, which reveal the fatty acid chain composition, correspond to PE 16:0_16:1 (precursor m/z 688), PG 16:0_16:1 (precursor m/z 719), and PG 16:0_18:1 (precursor m/z 747). A lower intensity feature is observed at (702, 267), corresponding to a PE lipid with a C_{17} fatty acid chain. A second feature is observed at (660, 283), potentially corresponding to PE 18:0_12:1, although the second fatty acid lipid is not observed elsewhere in the 2D MS/MS domain.

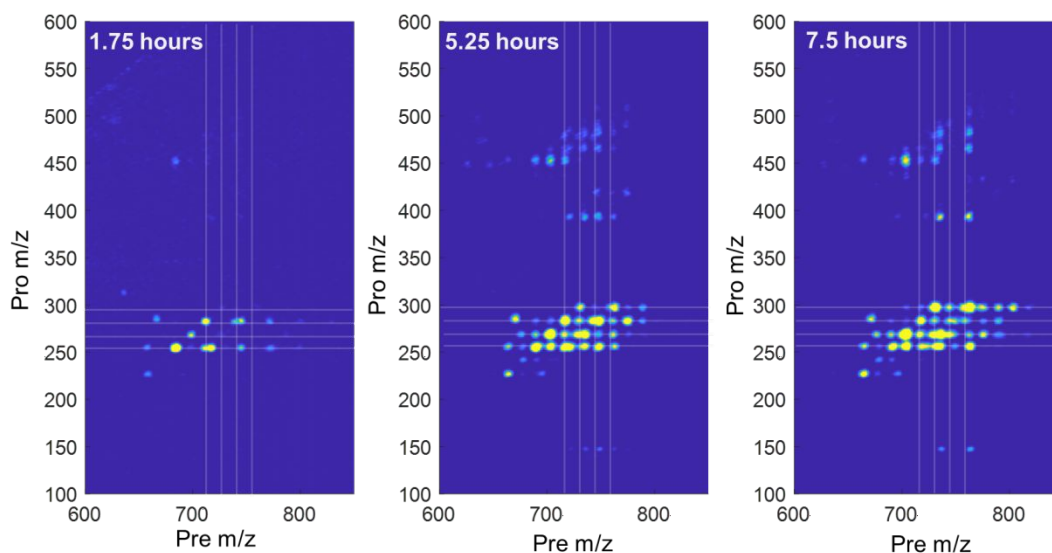
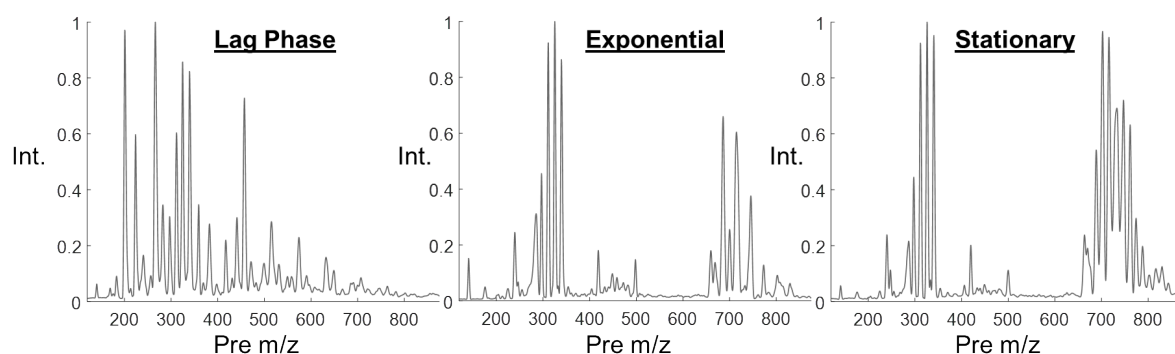


Figure 2. Lipid region of three 2D MS/MS spectra obtained from *E. coli* lysate over (left to right) at 1.75, 5.25, and 7.5 hours of growth. Product ions that fall on the same horizontal or diagonal lines are related by a common structural feature: they correspond to conventional MS/MS precursor and constant neutral loss scans. White vertical and horizontal lines are equally spaced approximately 14 mass units apart.

1
2
3 At 5.25 hours, which is near the end of the exponential phase, increased intensity is observed at (702,
4 255) and (702, 267), corresponding
5
6 to PE 16:0_17:1. Finally, at longer times, during the stationary phase, the shift to cyclopropyl PE's and
7
8 PG's continues, resulting in a distribution favoring odd-carbon number lipids over even-carbon lipids.
9
10 Individual 2D MS/MS mass spectra can be found in the time-lapse video in Figure S2.

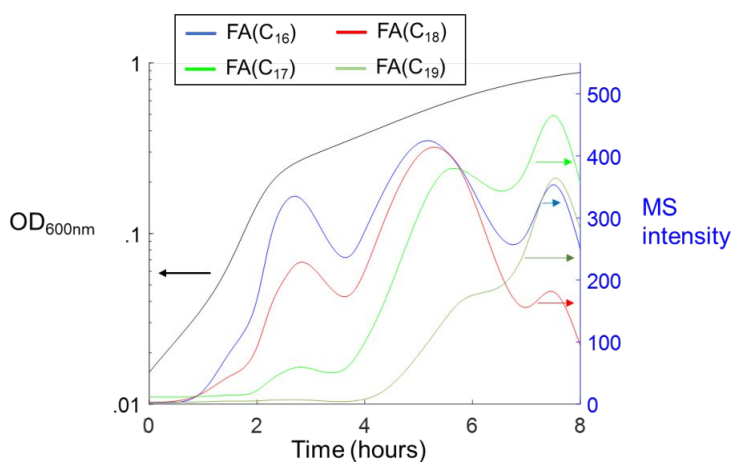
11 The 2D MS/MS data domains can be simplified by manipulating the 2D data. Extraction of
12 individual 1D lines from the 2D domain results in spectra identical to those obtained by the commonly
13 used MS/MS scan modes: product ion, precursor ion, and neutral loss scan. A much less common
14 operation is to project the data onto either the precursor or product ion axis so producing the anterior and
15 posterior mass
16
17 spectrum, respectively.³⁴ Whereas extraction of data removes data in order to observe specific functional
18
19 groups, the projection of data allows all data to be observed in a simpler form. By projecting all observed
20 ions to the precursor ion axis, the spectrum obtained (anterior mass spectrum) has axes which are
21 equivalent to those of a simple single-stage mass spectrum. The data in this form allows for gross
22 interpretation of molecular changes in the bacterium. The 2D MS/MS data domains shown in Figure 2, is
23 converted into the anterior mass spectra are shown in **Figure 3**. Note that the data observed in these
24 spectra are composed of ions detected after the activation of the precursor ion, viz. to product ions or
25 unfragmented precursor ions. A few key trends are observed. At early growth times the mass spectrum is
26 largely comprised of signals in the lower mass region, whilst phospholipids are in low abundance. As
27 growth progresses, the phospholipid region (m/z 650-850) shows increasing intensity. Furthermore, the
28 dominant phospholipid peaks shift over time towards higher m/z values. Such behavior is consistent with
29 the known *E. coli* lipid metabolic pathways, in which free fatty acids are phosphorylated and then
30 incorporated into phospholipids in a multi-step process.³⁵

31
32 In the phospholipid region, the most intense features at early times are at m/z 688, m/z 719, and
33
34 m/z 747. Analysis of these peaks, simply based upon their masses, gives putative assignments of PE 32:1,
35
36 PG 32:1, and PG 34:1, respectively.³⁶ At longer times, particularly towards the end of the exponential
37
38
39
40
41
42
43
44



57
58 **Figure 3.** Anterior mass spectrum (projected from 2D MS/MS mass spectrum) from *E. coli* lysate at log, exponential and
59 stationary stages of growth where fragments and residual precursor ions are observed at their respective precursor ion m/z
60

1
2
3 growth period, ions of m/z 702 and m/z 733 peaks increase in intensity relative to the other three peaks.
4 These peaks have masses consistent with PE 33:1 and PG 33:1, respectively. At longer times, the m/z 702
5 and m/z 733 become the dominant spectral features, along with a new feature at m/z 761 (putatively
6 assigned as PG 35:1). While the full scan MS provides some information about the lipids present, this
7 data lacks the detailed structural information about the side chain composition which is crucial for
8 phospholipid identification. For this information, the full 2D MS/MS data domain provides detailed
9 structural information. Since the major molecular change appears to be the conversion of alkenes into
10 cyclopropyl groups, this conversion can be monitored by extracting information pertaining to those two
11 functional groups. Specifically, the shift in distribution between even carbon number to odd carbon
12 number fatty acids can be simplified so that only lipids fatty acids with 16, 17, 18, or 19 carbons are
13 detected. The lipid data corresponding to the product ions of fatty acids of each chain length were
14 obtained from the 2D MS/MS scan and fitted to a curve and is shown in **Figure 4**. It can be seen that the
15 even carbon-number fatty acids (FA₁₆/FA₁₈) have intensities that follow optical density measurements
16 through the exponential phase. The odd-carbon number fatty acids (FA₁₇/FA₁₉) lag behind and begin at
17 the late exponential phase and continue into the stationary phase.



31
32
33
34
35
36
37
38
39
40
41
42
43
44
45
46 **Figure 4.** Fatty acid composition monitored over time detected by summing the product ion intensities corresponding to
47 different fatty acid chain lengths from the lipid mass region. The OD_{600nm} measurements are shown for comparison.

51 *DESI-2D MS/MS of Bacterial Extracts*

52
53 The nESI experiments just described are mainly limited by the time required for bacterial growth
54 (hours). However, this feature is specific to this experiment and many other analyses involving bacteria

will not be so constrained. The 2D MS/MS approach can be made even faster by using DESI instead of nano-electrospray experiments. In the latter, the analysis time per sample is 25 seconds, but significant time is spent moving from one sample to the next. In order to improve throughput, DESI was implemented so that the samples could be placed directly on a microscope slide and the time between samples could be reduced to under a second. This allowed a full 2D MS/MS scan (m/z 100 – m/z 900), both axes) to be recorded three times as fast as taken to record only the lipid region in the nESI experiment.

To demonstrate performance of the automated DESI-2D MS/MS system, cell lysate of *E. coli* was deposited onto four wells of a microscope slide and interrogated by DESI-2D MS/MS. **Figure 5a** shows the 2D MS/MS mass spectrum obtained from one of the wells containing the cell lysate acquired over approximately 5 seconds. The cell lysate analyzed in this experiment is from the stationary phase where most of the double bonds are converted to cyclopropyl groups resulting in a higher abundance of odd-carbon number lipids (PE/PG(33:1)). The ion chromatogram acquired while moving the DESI sprayer over all four wells is shown in **Figure 5b** where the extracted ion signal relates to a particular lipid present in *E. coli*. A time-lapse graphic displaying multiple 2D MS/MS spectra acquired by DESI can be found in Figure S3 where *E. coli* and *Pseudomonas aeruginosa* are analyzed in duplicate in a single run.

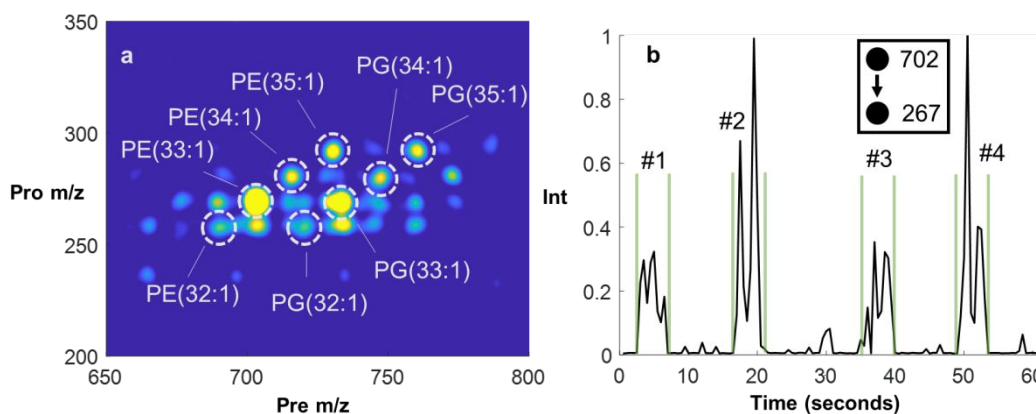


Figure 5. (a) 2D MS/MS mass spectrum obtained from automated DESI-2D MS/MS system. (b) Extracted ion signal corresponding to PE(33:1) recorded over time as four bacteria samples placed on a microscope slide are examined by DESI-MS.

To further illustrate how the DESI-2D MS/MS system can be used to interrogate a large number of samples, the bacterial growth of *E. coli* was again investigated. **Figure 6a** shows the resulting growth curve and extracted lipidomic information. Each of the twenty timepoints shown in **Figure 6a** contains 3 biological replicates with 3 scan replicates resulting in 180 unique spectra acquired in under 38 minutes (12.5 seconds a sample). It can be seen that the growth curve barely reaches the stationary phase resulting in smaller differences than observed in **Figure 4**. This can most likely be attributed to the differences in growth conditions although exact correlations cannot be made. The 2D MS/MS mass spectrum of the last

time point (570 minutes) is shown in **Figure 6b**. The conversion of C₁₆ to C₁₇ fatty acids is lower than what has been previously observed after the same time further confirming the reduced growth rate.

These DESI-MS data showcase two key advantages of the 2D MS/MS methodology, namely: i) the technique allows for data independent acquisition (DIA) by sampling all ions which fragment in a sample and ii) the short scan time to acquire all MS/MS data without chromatography allows for relatively high sample throughput. Furthermore, the extraction used for the growth curve monitored by DESI-2D MS/MS was not required in order to observe lipids. The spectrum acquired in **Figure 5a** was acquired from a bacterial sample without sample extraction. This experiment allows detailed insights into

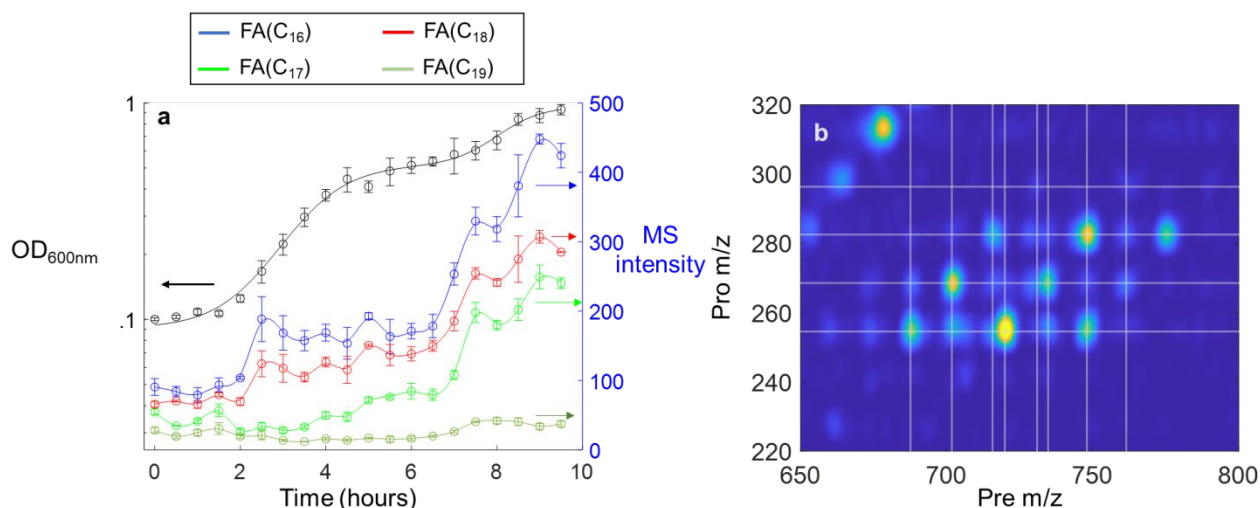


Figure 6. (a) Fatty acid composition monitored over time for three biological replicates under the same conditions. OD_{600nm} measurements are also shown. (b) DESI 2D MS/MS mass spectrum of lipid extract after 570 minutes of growth.

the changing lipidome. Lipids can have many structural isomers due to the possible combinations of fatty acid chains; this means that these structural isomers can be readily observed and identified although additional information in terms of double bond and sn-positional isomers is not acquired.

It can be seen that the mass resolution in the 2D MS/MS mass spectrum is poor (>5 Th in both axes) compared to more conventional MS/MS methods. This is due to the incredibly fast scan rate and the use of nitrogen as bath gas. Slower 2D MS/MS scans are possible with increased mass resolution and accuracy, but a quicker scan was chosen to emphasize speed. The major changes observed in this experiment, conversion of a double bond into a cyclopropyl group, do not necessitate higher mass resolution. However, the poor mass resolution does not allow distinction between different degrees of unsaturation for fatty acids with the same carbon number. Additionally, the more conventionally used helium could be substituted for the nitrogen bath gas to achieve higher mass resolution but at the cost of sensitivity. Another drawback of this method is the low dynamic range of the current detection circuitry (~2 orders of magnitude) caused by an exceptionally high electronic noise floor. With proper detection

1
2
3 electronics now being constructed, the dynamic range is expected to be four orders of magnitude. The
4 current instrument is still being improved so metrics such as resolving power and accuracy are not final
5 values.
6
7

8 9 **Conclusions**

10
11 The work presented here demonstrates a technique which leverages 2D MS/MS to make powerful
12 molecular measurements on biological mixtures without the need of chromatographic separation. The use
13 of ambient ionization provides high sample throughput as demonstrated by monitoring the growth of *E.*
14 *coli* by 2D MS/MS using two ionization methods, nano-electrospray ionization, and DESI. The lipid
15 profile of *E. coli* was monitored to observe a major lipidomic change, the conversion of double bond fatty
16 acids into cyclopropyl fatty acids. Importantly, this lipid profile shift was also monitored using high
17 throughput instrumentation where an entire 20-point growth curve with 9 replicates interrogated in under
18 38 minutes by DESI-2D MS/MS. The method gives insight into lipid modifications, specifically lipid
19 fatty acid chain modifications of unsaturated to cyclopropyl groups, with unprecedented speed.
20
21
22
23
24
25
26

27 **Conflicts of Interest**

28 There are no conflicts of interest to declare.
29
30

31 **Acknowledgements**

32
33 This material is based upon work supported by Teledyne FLIR under award 20089402, in
34 conjunction with Defense Threat Reduction Agency Project Agreement CWMD1916-004 on Base
35 Agreement CWMD 2018-841 and by the U.S. Department of Homeland Security under Grant Award
36 Number 20CWDAR100039-01. Nicolás M. Morato acknowledges support from the American Chemical
37 Society Division of Analytical Chemistry Graduate Fellowship sponsored by Agilent Technologies. Mark
38 Carlsen and Mike Everly (Jonathan Amy Facility for Chemical Instrumentation at Purdue University) are
39 acknowledged for their modifications to the mass spectrometer and data acquisition software.
40
41
42
43
44
45
46
47
48
49
50
51
52
53
54
55
56
57
58
59
60

References

- 1 (1) Henderson, J. C.; Zimmerman, S. M.; Crofts, A. A.; Boll, J. M.; Kuhns, L. G.; Herrera, C.
2 M.; Trent, M. S. *Annu. Rev. Microbiol.* **2016**, *70* (1), 255–278.
- 3 (2) Lin, T.-Y.; Weibel, D. B. *Appl. Microbiol. Biotechnol.* **2016**, *100* (10), 4255–4267.
- 4 (3) Barák, I.; Muchová, K. *Int. J. Mol. Sci.* **2013**, *14* (2), 4050–4065.
- 5 (4) Magnuson K; Jackowski S; Rock C O; Cronan J E. *Microbiol. Rev.* **1993**, *57* (3), 522–542.
- 6 (5) Jeucken, A.; Molenaar, M. R.; van de Lest, C. H. A.; Jansen, J. W. A.; Helms, J. B.;
7 Brouwers, J. F. *Cell Rep.* **2019**, *27* (5), 1597-1606.e2.
- 8 (6) Furse, S.; Wienk, H.; Boelens, R.; de Kroon, A. I. P. M.; Killian, J. A. *FEBS Lett.* **2015**,
9 *589* (19, Part B), 2726–2730.
- 10 (7) Jarmusch, A. K.; Pirro, V.; Baird, Z.; Hattab, E. M.; Cohen-Gadol, A. A.; Cooks, R. G.
11 *Proc. Natl. Acad. Sci.* **2016**, *113* (6), 1486.
- 12 (8) Czamara, K.; Majzner, K.; Selmi, A.; Baranska, M.; Ozaki, Y.; Kaczor, A. *Sci. Rep.* **2017**,
13 *7* (1), 40889.
- 14 (9) Minamikawa, T.; Ichimura-Shimizu, M.; Takanari, H.; Morimoto, Y.; Shiomi, R.;
15 Tanioka, H.; Hase, E.; Yasui, T.; Tsuneyama, K. *Sci. Rep.* **2020**, *10* (1), 18548.
- 16 (10) Zhang, C.; Boppart, S. A. *Anal. Chem.* **2020**, *92* (24), 15943–15952.
- 17 (11) Fu, D.; Yu, Y.; Folick, A.; Currie, E.; Farese, R. V.; Tsai, T.-H.; Xie, X. S.; Wang, M. C.
18 *J. Am. Chem. Soc.* **2014**, *136* (24), 8820–8828.
- 19 (12) Lin, H.; Lee, H. J.; Tague, N.; Lugagne, J.-B.; Zong, C.; Deng, F.; Shin, J.; Tian, L.;
20 Wong, W.; Dunlop, M. J.; Cheng, J.-X. *Nat. Commun.* **2021**, *12* (1), 3052.
- 21 (13) Zhu, C.; Shi, W.; Daleke, D. L.; Baker, L. A. *Analyst* **2018**, *143* (5), 1087–1093.
- 22 (14) Cajka, T.; Fiehn, O. *TrAC Trends Anal. Chem.* **2014**, *61*, 192–206.
- 23 (15) Vasilopoulou, C. G.; Sulek, K.; Brunner, A.-D.; Meitei, N. S.; Schweiger-Hufnagel, U.;
24 Meyer, S. W.; Barsch, A.; Mann, M.; Meier, F. *Nat. Commun.* **2020**, *11* (1), 331.
- 25 (16) Song, Y.; Talaty, N.; Tao, W. A.; Pan, Z.; Cooks, R. G. *Chem. Commun.* **2007**, No. 1, 61–
26 63.
- 27 (17) Meetani, M. A.; Shin, Y.-S.; Zhang, S.; Mayer, R.; Basile, F. *J. Mass Spectrom.* **2007**, *42*
28 (9), 1186–1193.
- 29 (18) Cronan, J. E., Jr. *J. Bacteriol.* **1968**, *95* (6), 2054–2061.
- 30 (19) Arneborg, N.; Salskov-Iversen, A. S.; Mathiasen, T. E. *Appl. Microbiol. Biotechnol.* **1993**,
31 *39* (3), 353–357.
- 32 (20) Gidden, J.; Denson, J.; Liyanage, R.; Ivey, D. M.; Lay, J. O. *Int. J. Mass Spectrom.* **2009**,
33 *283* (1–3), 178–184.
- 34 (21) Gillet, L. C.; Navarro, P.; Tate, S.; Röst, H.; Selevsek, N.; Reiter, L.; Bonner, R.;
35 Aebersold, R. *Mol. Amp Cell. Proteomics* **2012**, *11* (6), O111.016717.
- 36 (22) Bateman, K. P.; Castro-Perez, J.; Wrona, M.; Shockcor, J. P.; Yu, K.; Oballa, R.; Nicoll-
37 Griffith, D. A. *Rapid Commun. Mass Spectrom.* **2007**, *21* (9), 1485–1496.
- 38 (23) Pfändler, P.; Bodenhausen, G.; Rapin, J.; Houriet, R.; Gäumann, T. *Chem. Phys. Lett.*
39 **1987**, *138* (2), 195–200.
- 40 (24) Paris, J.; Morgan, T. E.; Marzullo, B. P.; Wootton, C. A.; Barrow, M. P.; O'Hara, J.;
41 O'Connor, P. B. *J. Am. Soc. Mass Spectrom.* **2021**, *32* (7), 1716–1724.
- 42 (25) Szalwinski, L. J.; Cooks, R. G. *Talanta Open* **2021**, *3*, 100028.
- 43 (26) Blevins, M. S.; James, V. K.; Herrera, C. M.; Purcell, A. B.; Trent, M. S.; Brodbelt, J. S.
44 *Anal. Chem.* **2020**, *92* (13), 9146–9155.
- 45 (27) Li, Z.; Cheng, S.; Lin, Q.; Cao, W.; Yang, J.; Zhang, M.; Shen, A.; Zhang, W.; Xia, Y.;
46 Ma, X.; Ouyang, Z. *Nat. Commun.* **2021**, *12* (1), 2869.
- 47
48
49
50
51
52
53
54
55
56
57
58
59
60

- 1
2
3 (28) Zhang, X.; Ren, X.; Chingin, K.; Xu, J.; Yan, X.; Chen, H. *Anal. Chim. Acta* **2020**, *1139*,
4 146–154.
5 (29) Claes, B. S. R.; Bowman, A. P.; Poad, B. L. J.; Young, R. S. E.; Heeren, R. M. A.;
6 Blanksby, S. J.; Ellis, S. R. *Anal. Chem.* **2021**, *93* (28), 9826–9834.
7 (30) Snyder, D. T.; Cooks, R. G. *J. Am. Soc. Mass Spectrom.* **2017**, *28* (9), 1929–1938.
8 (31) Szalwinski, L. J.; Holden, D. T.; Morato, N. M.; Cooks, R. G. *Anal. Chem.* **2020**, *92* (14),
9 10016–10023.
10 (32) Sündermann, A.; Eggers, L. F.; Schwudke, D. In *Encyclopedia of Lipidomics*; Wenk, M.
11 R., Ed.; Springer Netherlands: Dordrecht, 2016; pp 1–4.
12 (33) Wei, C.; Zhao, X. *Front. Microbiol.* **2018**, *9*, 2728.
13 (34) Schwartz, J. C.; Wade, A. P.; Enke, C. G.; Cooks, R. G. *Anal. Chem.* **1990**, *62* (17), 1809–
14 1818.
15 (35) Zhang, Y.-M.; Rock, C. O. *Nat. Rev. Microbiol.* **2008**, *6* (3), 222–233.
16 (36) LMSD: LIPID MAPS® structure database. Sud M., Fahy E., Cotter D., Brown A., Dennis
17 E., Glass C., Murphy R., Raetz C., Russell D., and Subramaniam S., *Nucleic Acids*
18 *Research* *35*, D527-32 (2006).
19
20
21
22
23
24
25
26
27
28
29
30
31
32
33
34
35
36
37
38
39
40
41
42
43
44
45
46
47
48
49
50
51
52
53
54
55
56
57
58
59
60

Figures

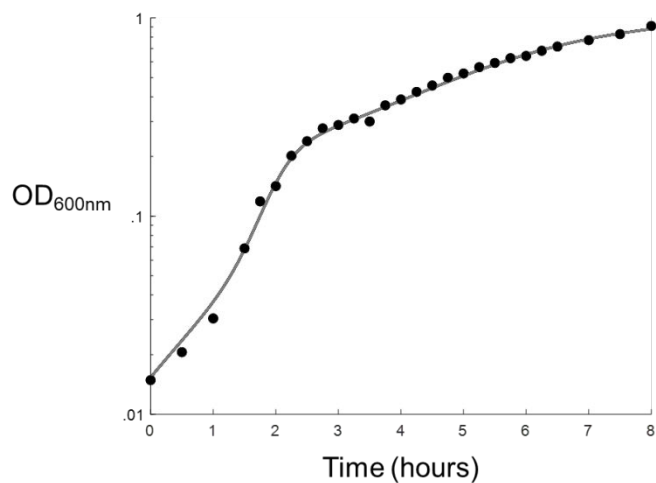


Figure 1. Optically measured growth curve of *E. coli* in LB medium at 37 °C

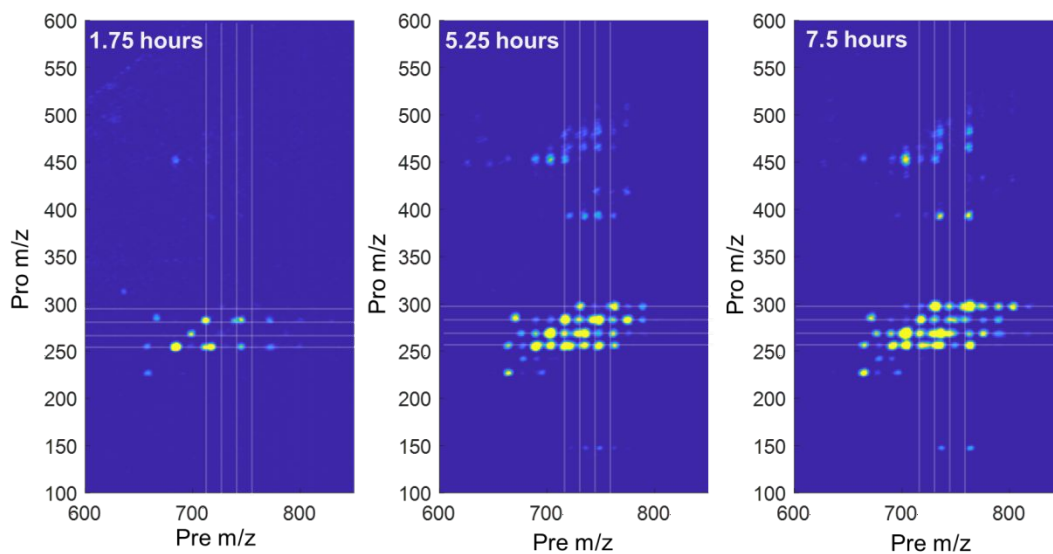


Figure 2. Lipid region of three 2D MS/MS spectra obtained from *E. coli* lysate over (left to right) at 1.75, 5.25, and 7.5 hours of growth. Product ions that fall on the same horizontal or diagonal lines are related by a common structural feature. White vertical and horizontal lines are equally spaced approximately 14 mass units apart.

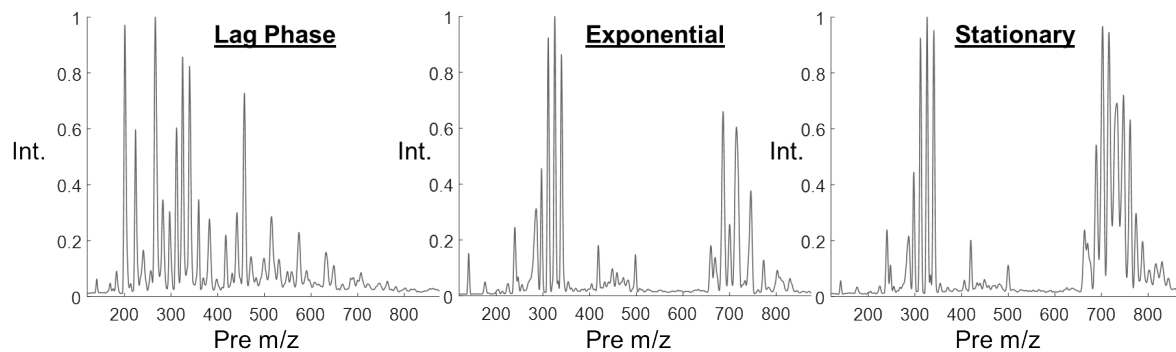


Figure 3. Anterior mass spectrum (projected from 2D MS/MS mass spectrum) from *E. coli* lysate at log, exponential and stationary stages of growth where fragments and residual precursor ions are observed at their respective precursor ion m/z values.

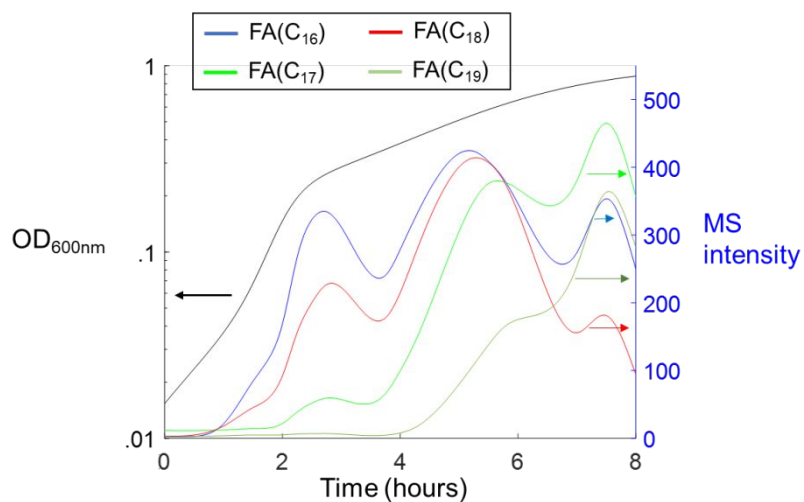


Figure 4. Fatty acid composition monitored over time detected by summing the product ion intensities corresponding to different fatty acid chain lengths from the lipid mass region. The OD_{600nm} measurements are shown for comparison.

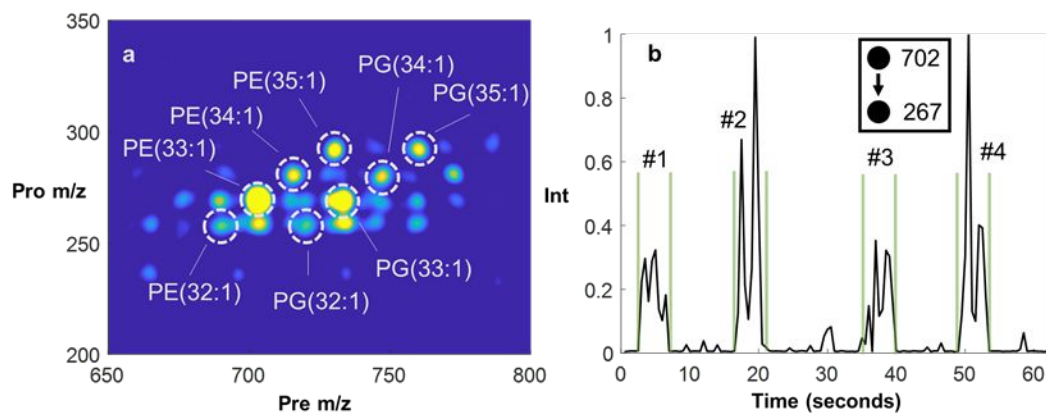


Figure 5. (a) 2D MS/MS mass spectrum obtained from automated DESI-2D MS/MS system. (b) Extracted ion signal corresponding to PE(33:1) over analysis time for the four bacteria samples placed on a 12-well microscope slide.

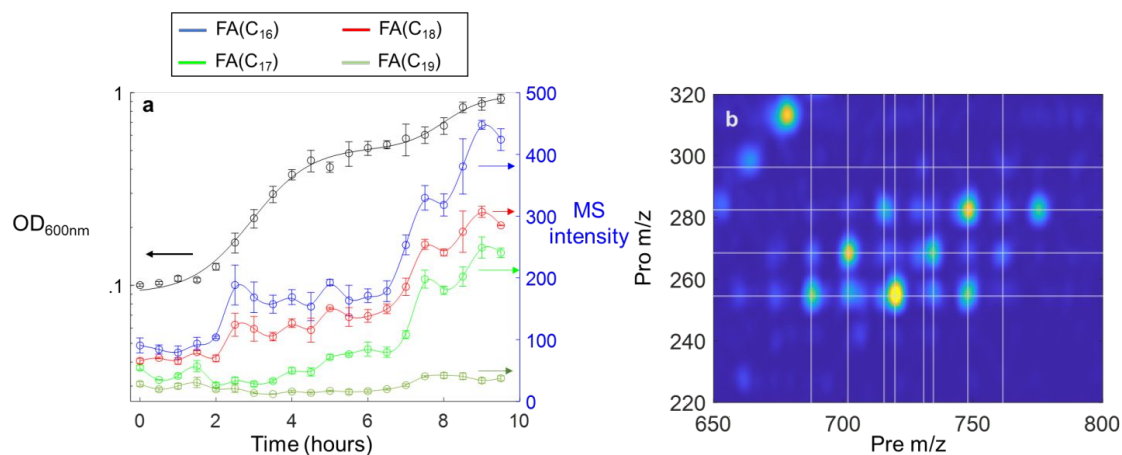


Figure 6. (a) Fatty acid composition monitored over time for three biological replicates grown under the same conditions. OD_{600nm} measurements are also shown. (b) 2D MS/MS mass spectrum of lipid extract after 570 minutes of growth.